Article

Streamflow Simulation in Semiarid Data-Scarce Regions: A Comparative Study of Distributed and Lumped Models at Aguenza Watershed (Morocco)

Abdelmounim Bouadila [1], Ismail Bouizrou [1], Mourad Aqnouy [2,3], Khalid En-nagre [3], Yassine El Yousfi [4], Azzeddine Khafouri [5], Ismail Hilal [6], Kamal Abdelrahman [7], Lahcen Benaabidate [1], Tamer Abu-Alam [8,9,*], Jamal Eddine Stitou El Messari [3] and Mohamed Abioui [10,11,*]

[1] Laboratory of Functional Ecology and Environmental Engineering, Department of Environment, Faculty of Sciences and Techniques, Sidi Mohamed Ben Abdellah University, Fez 30000, Morocco
[2] Applied Geology Research Laboratory—AGRSRT, Department of Geosciences, Faculty of Sciences and Techniques, Moulay Ismail University of Meknes, Errachidia 52000, Morocco
[3] Department of Earth Sciences, Faculty of Sciences, Abdelmalek Essaadi University, Tétouan 416, Morocco
[4] Environmental Management and Civil Engineering Team—ENSAH, Abdelmalek Essaadi University, Tétouan 93030, Morocco
[5] Laboratory of Geoheritage, Geoenvironment and Prospecting of Mines & Water, Department of Earth Sciences, Faculty of Sciences, Mohammed Premier University, Oujda 60000, Morocco
[6] Centre National de l'Energie, des Sciences et des Techniques Nucléaires (CNESTEN), Rabat 10001, Morocco
[7] Department of Geology & Geophysics, College of Science, King Saud University, Riyadh 11451, Saudi Arabia
[8] The Faculty of Biosciences, Fisheries and Economics, UiT The Arctic University of Norway, 9037 Tromsø, Norway
[9] OSEAN—Outermost Regions Sustainable Ecosystem for Entrepreneurship and Innovation, University of Madeira, Colégio dos Jesuítas, 9000-039 Funchal, Portugal
[10] Geosciences, Environment and Geomatics Laboratory (GEG), Department of Earth Sciences, Faculty of Sciences, Ibnou Zohr University, Agadir 80000, Morocco
[11] MARE-Marine and Environmental Sciences Centre—Sedimentary Geology Group, Department of Earth Sciences, Faculty of Sciences and Technology, University of Coimbra, 3030-790 Coimbra, Portugal
* Correspondence: tamer.abu-alam@uit.no (T.A.-A.); m.abioui@uiz.ac.ma (M.A.)

Abstract: In semi-arid regions such as the southwestern zone of Morocco, better management of water resources is crucial due to the frequent flooding phenomena. In this context, the use of hydrological models is becoming increasingly important, specifically in the Aguenza watershed. A multitude of hydrological models are available to make very efficient modeling, and from this perspective, a comparative approach was adopted using two models with different characteristics. Streamflow simulations were carried out continuously at daily time steps using GR4J and ATHYS (2002–2011). The latter was used also to simulate rainfall-runoff events (1984–2014). Simulation results using the distributed model are very efficient compared to those obtained by the lumped model "GR4J", which shows the disadvantages of neglecting the hydrological processes during a hydrological study. However, a remarkable improvement was observed in the general appearance of the resulting hydrographs and the performance parameters after using the distributed model ((Calibration: NSE, RSR, and PBIAS increased successively by 8%, 6%, and 45.2%); (Validation: NSE, RSR, and PBIAS increased successively by 6%, 4%, and 8.9%)). In terms of flood event simulations, a good concordance between observed and simulated discharge was observed ($NSE_{median} = 0.7$), indicating its great reliability for simulating rainfall-runoff events in semi-arid and data-scarce regions. This research highlights the importance of using hydrological models, specifically the distributed model ATHYS, for the better management of water resources in semi-arid regions with frequent flooding events.

Keywords: semi-arid region; Aguenza watershed; distributed model "ATHYS"; lumped model "GR4J"; continuous and event-based modeling

1. Introduction

Water resource availability is directly connected to the sustainability and development of human society and ecosystems [1–3]. Due to limited water supplies and pressure from increasing water consumption, water resources are becoming scarcer, especially in arid and semi-arid environments [4–9]. As a result, hydrological patterns, particularly in these climatic zones, are likely to be affected. Therefore, these regions are likely to face the greatest pressure in freshwater supply and management [10–13]. In addition, there is an urgent need to characterize the rapid response of runoff to extreme precipitation events that are becoming more frequent in arid and semi-arid and Mediterranean regions [14,15], as they often generate extremely damaging flash floods and inundations [16–18]. Since accurate simulations of flow are possible in arid and semi-arid regions, effective water resource management and flood warning require accurate and precise simulations of streamflow [19–25].

Hydrological modeling in semi-arid areas is strongly influenced by alternating seasons [26,27]. These studies have shown that the flow regime of rivers in these contexts is largely influenced by a highly variable distribution of precipitation during the seasons; i.e., maximum flows are generally observed in winter, autumn, and sometimes spring, while low-flow periods are most often marked during the dry period of the year, namely "summer". During the last decades, hydrological modeling has undergone a long process of improvement through the development of advanced models that differ in terms of temporal classification of space and processes and integrate the complexity of the system in hydrological simulations. In addition, modeling has become one of the main tools for water resources management since extreme events (floods and droughts) are more devastating and threaten the population worldwide [28–32]. It is noteworthy that the improvement of the performance of flow simulations in semi-arid regions is necessary, and this can only be done through the implementation of models more suitable for these areas, especially the discrete, semi-distributed, and global conceptual models that are most used in hydrological studies due to their adaptability to different climatic contexts [33–35]. This applicability usually differs from one climate to another, and even within the same climate, one can sometimes have very different results from one period to another [36–45]. Conceptual hydrological models offer several advantages in terms of applicability, especially in developing country basins that are characterized by data scarcity [46–48]. Among their advantages are the reduced number of data inputs and consequently a reduced number of calibrated parameters of hydrological models. This is known to be effective for avoiding overparameterization risk and reducing the model uncertainty issue [49]. Based on these advantages, the applicability of these conceptual models to a wide range of watersheds around the world can be easily justified.

In this study, a comparative hydrological modeling approach was adopted through the use of two models with different levels of sophistication: the distributed model (ATHYS) [50] and the lumped model (GR4J) developed by CEMAGREF [51]. The ATHYS model was based on a variety of production and transfer methods. The runoff from each grid cell was computed using a reservoir model, and the runoff volume was routed to the outlet using a lag and route routing method to obtain the hydrograph and volume of the discharge. The main advantage of the GR4J model is that it does not require a comprehensive description of the watershed and its continuous functioning, ensuring throughout the year a complete accounting of the water entering and leaving the basin and monitoring the overall humidity level [52]. The input data are precipitation and evapotranspiration, which are simple measurements with few parameters to be adjusted.

The region of Souss-Massa (southwest Morocco), including the Aguenza watershed, which is the subject of this study, presents a great constraint, that could be a limiting factor if not a brake of its development: the problem of floods and inundations. Indeed, this watershed is one of the Moroccan watersheds that contain a large number of sites threatened by floods. The latter sometimes disrupts the economic activities of this basin and causes considerable damage to the basic infrastructures and also to agricultural

production, which is the main source for most inhabitants in these regions [53]. During this study, two modeling approaches were used to understand better the hydrological behavior of the Aguenza watershed. The first approach consists of using daily data to carry out continuous modeling that allows us to better analyze the fast-evolution inflows after the rainstorms. Generally, this approach is considered the most appropriate since it takes into account for each event the previous rainfall (previous 10 days) in determining the parameters. Furthermore, continuous hydrological models are considered the most appropriate for estimating initial conditions [54,55]. In this sense, the continuous approach has some disadvantages concerning the data series used; i.e., it needs to provide long precipitation time series and, in some cases, other data such as evapotranspiration, temperature, relative soil moisture, etc. [56]. The continuous mode simulation uses two conceptual rainfall-runoff models that differ in terms of spatialization to test their influence on the quality of results. The second phase of this study consisted of using the most important historical flood events that occurred in the Aguenza watershed either in autumn or winter between 1984 and 2014 in order to elaborate an event-based modeling (time step = 60 min). Indeed, ten of the most intense rainfall-runoff events (maximum rainfall intensity reaching in the studied basin a value of 13.20 mm·h^{-1}) were used to study and simulate the hydrological behavior of the Aguenza watershed, in particular the flood-generation process.

The main objectives of the present study are the following: (1) comparing distributed and lumped models to evaluate the utility of using a spatially distributed modeling approach for correctly reproducing the Aguenza streamflow continuously at daily time steps and (2) using the event-based mode to characterize the flood-generation process by simulating historical rainfall-runoff events. Our findings are expected to provide water managers with valuable information for better water resource management and subsequently for establishing preventive measures.

2. Materials and Methods

2.1. Study Area

The general context of the study is part of a comprehensive framework that includes the full extent of the land affected by the flood problem, namely the Souss Plain that is part of the large Souss-Massa Basin. The origin of floods comes from the various tributaries of the Souss Basin, which have violent and irregular floods. Therefore, it is the Souss Basin and more precisely the station of the Aguenza watershed that is the subject of this study. The Aguenza watershed covers an area of 1162 km^2 (Figure 1). The Anti-Atlas Mountains from the southern part and the High-Atlas Mountains, which constitute the eastern and northern parts of the watershed, delimit it. In terms of climate, the river is dominated by arid to semi-arid climates, with the heaviest precipitation falling on the upper Atlas outcrops [57]. The mean annual precipitation varies from 280 mm in the Anti-Atlas downstream part to 600 mm, which is observed in the High Atlas Mountains upstream part.

2.2. Data Processing

2.2.1. Geographic Data

The digital elevation model (DEM) is a set of altimetric points (three coordinates: x, y, and z). The assembly of these points makes it possible to reconstitute the topography of the site; note that, in this study, a DEM with a high resolution of 12.5 m was used. The software then processes these data to obtain the hydrographic network, the sub-watersheds, the drainage directions, etc. (Figure 2). In addition, to have correct results, it is necessary to make some corrections, especially for the drainage files (depression and loop correction).
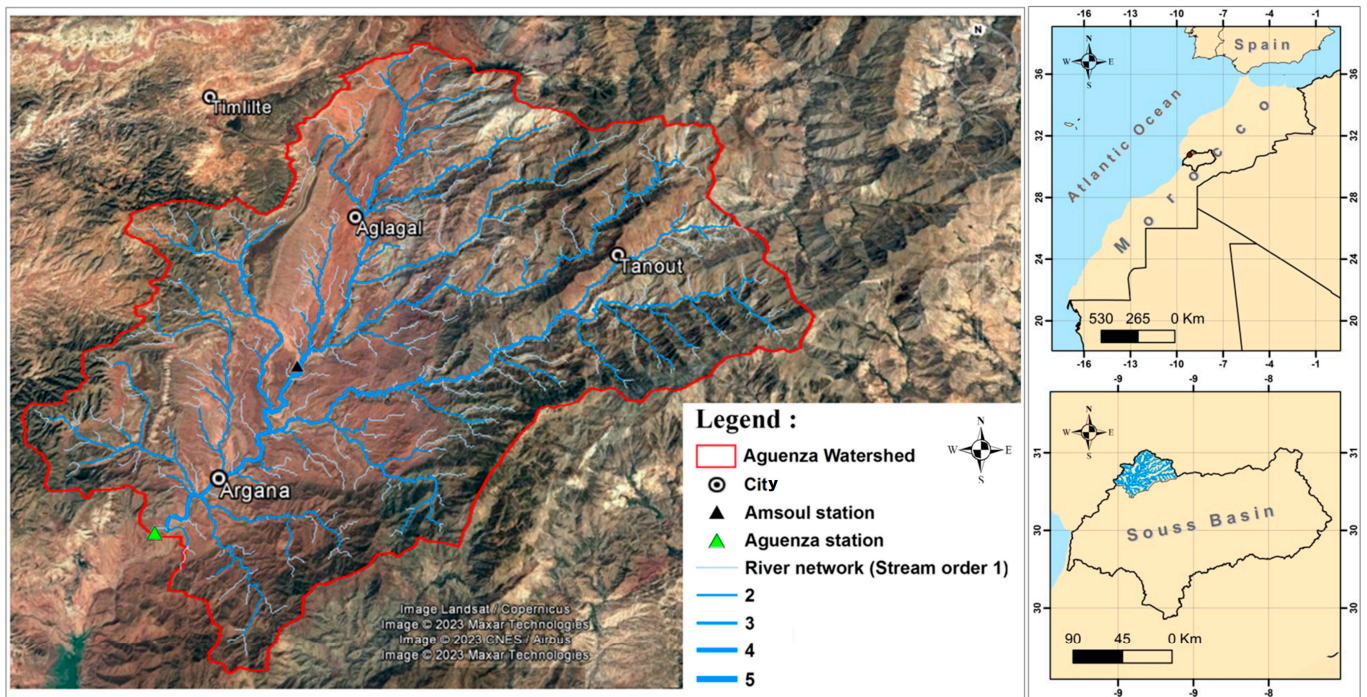
Figure 1. Location of the Aguenza watershed, Morocco.
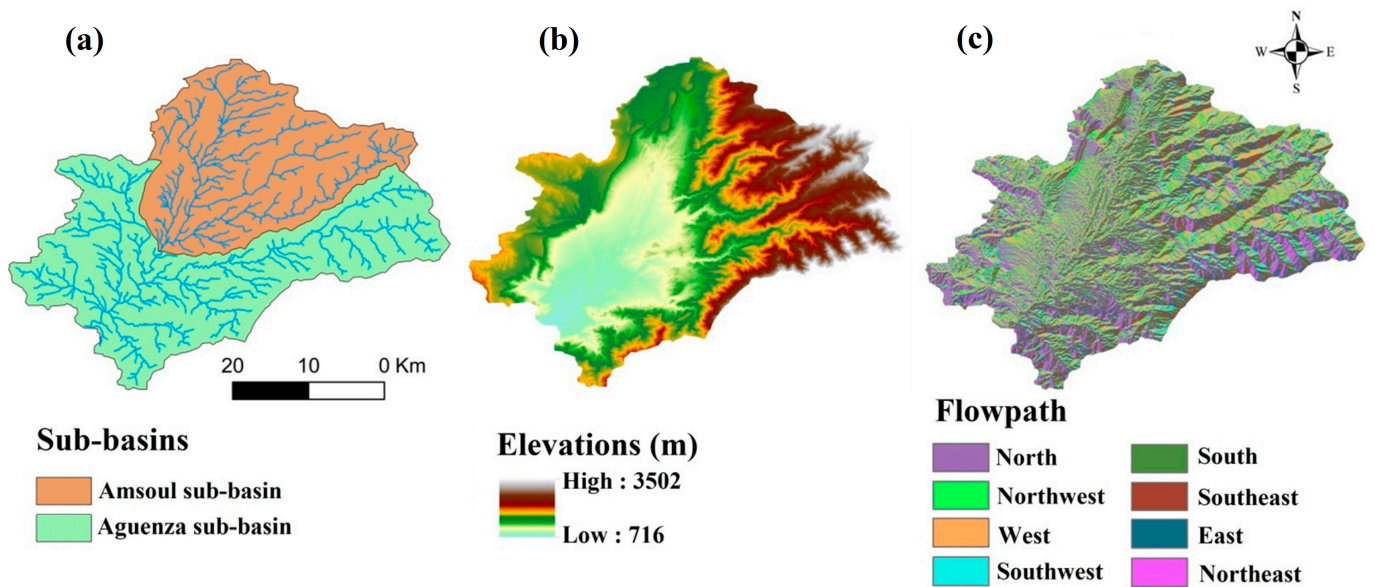
Figure 2. (**a**)The hydrographical network map with the sub-basins, (**b**) altitude map of Aguenza watershed; (**c**) drainage directions map.

2.2.2. Meteorological Data

In this study, daily precipitation, temperature, and evapotranspiration (from 1 January 1982 to 31 December 2011) were obtained for two meteorological stations (Aguenza and Amsoul), and flow data series were obtained for one flow gauge (Aguenza: from 1 January 2000 to 31 December 2011). It is also important to note that the hydro-meteorological data were obtained on an hourly time step to perform an event study focusing on the ten most significant flood events that occurred in the Aguenza watershed between the years 1984 and 2014.

The Aguenza watershed is characterized by a rainy season and a hot and dry summer with an average of 271.34 mm/year (1982–2011). Two seasons can be distinguished:

the rainy season (October to April) with irregular rainfall and the dry season (May to September) where precipitation is relatively low (Figure 3). The temperature regime is characterized by strong annual amplitudes that accentuate the phenomenon of evapotranspiration. The annual evaporation is 2279 mm. Evaporation is highest in July (360 mm) and lowest in December and January (46 mm).

Figure 3. Ombrothermal diagram of the Aguenza watershed for the observation period: 1982–2011 (scale: P = 2 T).

2.3. ATHYS Platform

ATHYS is a rainfall-runoff modeling platform developed by the Research Institute for Development (IRD) in Montpellier, France; it consists of four modules: (i) MERCEDES (Regu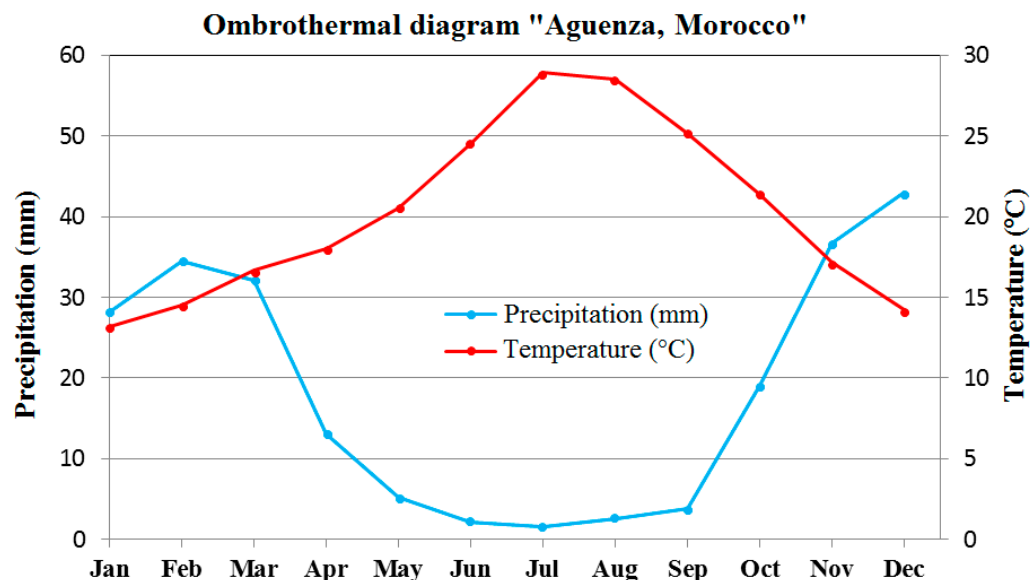lar Square Elementary Mesh for the Study of Superficial Flows); (ii) VISHYR (Visualization of Hydrological data); (iii) VICAIR (Visualization of Raster Maps and Images); and (iv) SPATIAL: spatial interpolation platform [58]. MERCEDES is based on the spatial discretization of the basin in regular square meshes, which makes it possible to take into account the spatial variability of the main factors that determine the flows [59]; the main interest of this free software is the possibility to spatialized the rainfall–runoff transformation. Indeed, the model uses a DEM as input to calculate the runoff mesh by mesh. This principle is combined with a spatialization of rainfall data, which allows large catchments to account for spatial variation of rainfall intensities. The flow generated for a rainy event (rainfall–runoff transformation) is calculated in three steps (Figure 4):

- For each mesh, the production model is used to estimate the amount of rain that contributes to runoff;
- The transfer model calculates the hydrograph produced by each mesh at the outlet of the catchment. This calculation is made from the result obtained by applying the production function;
- The inputs of each mesh are summed to obtain the total flow at the outlet.

From the input data (DEM, drainage file, and precipitation), the ATHYS hydrological model allows to definition of the streamflow at the daily and hourly time step in various points of the catchment.

The software offers several production and transfer models. The following choices were made.
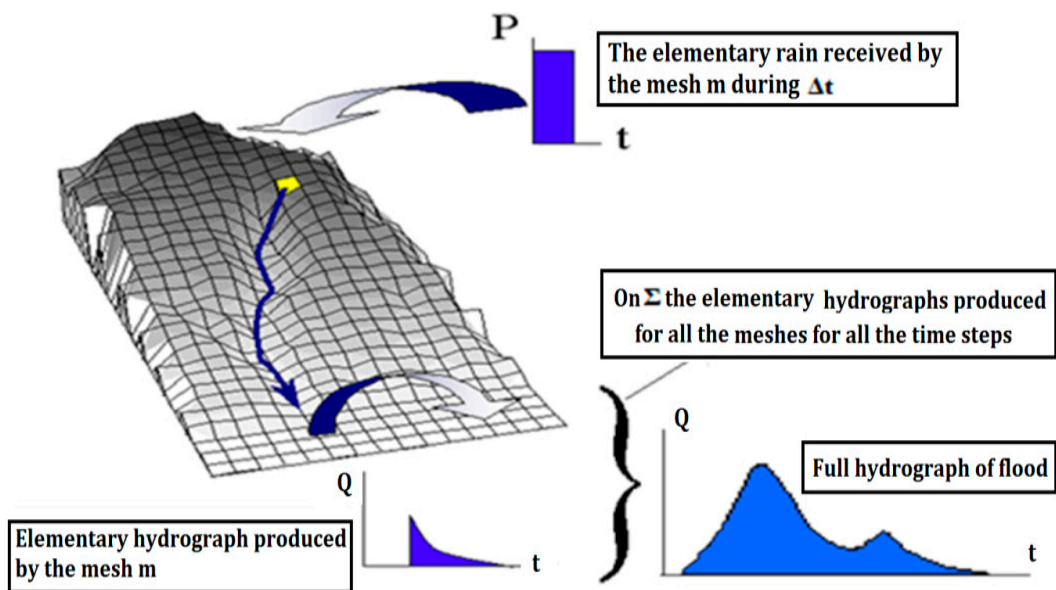
Figure 4. Functioning of the ATHYS model (www.athys-soft.org, accessed on 15 March 2022).

2.3.1. Production Function "SCS"

The U.S. Department of Agriculture Soil Conservation Service (USDA-SCS) model [60] was selected as a production function to estimate the precipitation amounts that contribute to the runoff generation. This function was extensively used in successively applied in a semi-arid environment, including the Moroccan basins [19,20,33,61,62]. The SCS principle of functioning is illustrated in Figure 5. For each square mesh of the watershed discretization, a ground tank is associated. The capacity of this soil reservoir defines the initial water deficit of the mesh: this parameter is denoted as S (mm). It is the function of the initial water content in the soil and the maximum storage capacity of local water when the soils are dry, or at least, very little moist. This parameter constitutes the initial condition of the model and is variable from one event to another. The SCS model is particularly sensitive to the capacity of this soil reservoir [57,63].
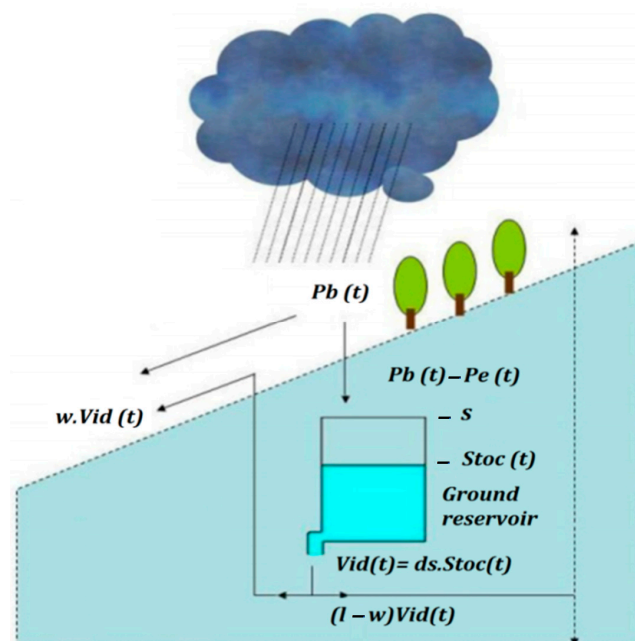
Figure 5. Principle of the SCS production function (www.athys-soft.org, accessed on 15 March 2022).

The SCS method is the most commonly used and is capable of fitting different types of flooding processes [60]. The version used in this study is composed of three parameters:

- S (mm) represents the total capacity of the ground tank, and this capacity depends on many characteristics of the soil (depth, heterogeneity, porosity, hydraulic conductivity, a dip of the subsoil, etc.);
- ds (d^{-1}) is the proportional emptying at the level of the reservoir by deep percolation, evaporation, sub-surface flow, etc.;
- ω (dimensionless) represents the fraction of drainage, which participates in the runoff in the form of exfiltration.

2.3.2. Transfer Function "Lag and Route"

The choice of the lag and route model is explained by the desire to obtain both global modelings in the contribution of different parameters (losses, runoff, etc.) and precision by choosing to know this contribution for each mesh independently of the others (Figure 6).
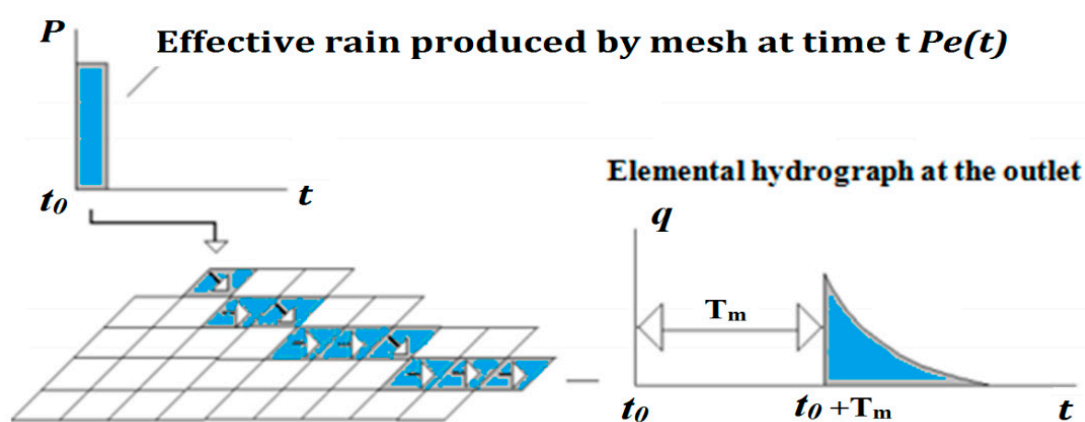
Figure 6. Routing model operating for each mesh of the basin (www.athys-soft.org, accessed on 15 March 2022).

Moreover, in this model, all parameters are constant over time. This function consisted of the two following parameters:

- V_0 (m/s) is the maximum velocity reached at the outlet during the event. This model calculates a transfer time Tm that designates the time elapsed between the rain falling on the mesh m and the start of the passage of the event in the outlet. It is calculated from the position of the mesh and the outlet (length Lm between mesh and outlet), the drainage pattern, and the speed V_0;
- K_0 (dimensionless) is called the damping parameter. It is connected to the damping time Km by the following relationship:

$$Km = Ko \times Tm \tag{1}$$

2.4. GR4J Model

The GR4J model is a four-parameter rainfall–runoff transformation model [51]. The version used was developed by Perrin in 2002 and improved by Perrin and his team in 2003. The GR4J model is characterized by a structure with two associated tanks (Figure 7): the first tank is a production tank, and the second is a routing tank; these are linked to unit hydrographs (SH1 and SH2) to obtain finally a simulated flow (expressed in mm) as an output of the model. This model also allows monitoring of the pond's moisture status to take into account previous conditions and ensure continuous operation [64].
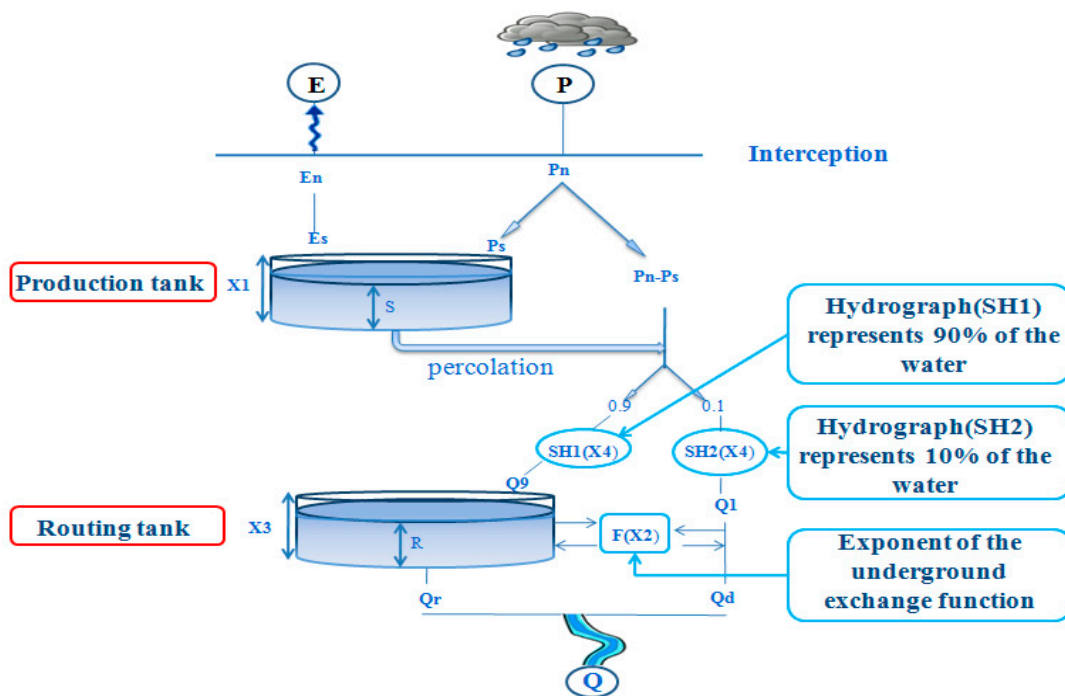
Figure 7. Structure diagram of the new version of the GR4J model.

The GR4J model is a global model with four parameters, and these parameters are as follows:

X1: Maximum capacity of the production tank (in mm);
X2: Coefficient of the underground exchange function (in mm);
X3: Maximum capacity of the routing tank (in mm);
X4: Base time of the unit hydrograph (days);
Input data: Daily precipitation and evapotranspiration (mm/d);
Data produced average daily flow (mm/d).

2.5. Performance Criteria

The performance criteria of a hydrological model can be based on mere visual appreciation or based on statistical calculations known as objective functions to standardize the comparison between the result of the simulation or forecast and observations [65]. The identification of the parameter values of the hydrological model, depending on the objective function used, quantifies the difference between the observed and simulated variables. The most commonly used objective function in hydrology is the Nash–Sutcliffe criterion (NSE), and closer the latter is to 1, the closer the simulation is to the observation [66]:

$$\text{NSE} = 1 - \frac{\sum_{i=1}^{n}(\text{Qobs, i} - \text{Qcalc, i})^2}{\sum_{i=1}^{n}(\text{Qobs, i} - \text{Qobs, m})^2} \tag{2}$$

The determination coefficient (R^2) was also used in this study. This criterion varies between 0 and 1 (a value of 1 indicates that the simulation is identical to the observation). The mathematical equation describing this criterion is as follows:

$$R^2 = \frac{\sum_{i=1}^{n}(\text{Qobs, i} - \text{Qobs, m}) \cdot (\text{Qcalc, i} - \text{Qcalc, m})}{\sqrt{\sum_{i=1}^{n}(\text{Qobs, i} - \text{Qobs, m})^2} \cdot \sqrt{\sum_{i=1}^{n}(\text{Qcalc, i} - \text{Qcalc, m})^2}} \tag{3}$$

However, the RMSE-observations standard deviation ratio (RSR) is also used to evaluate the performance of the model. The use of this standard deviation (SD) of the observed data allows the normalization of the RMSE criterion. It is frequently used to measure the

differences between the values predicted by a model and the observed values [67–69]. Its range varies from 0 to infinity, while a value of 0 is a perfect score. It is given as follows:

$$\text{RSR} = \frac{\text{RMSE}}{\text{STDEV obs}} = \sqrt{\frac{\sum_{i=1}^{n}(\text{Qobs, i} - \text{Qcalc, i})^2}{\sum_{i=1}^{n}(\text{Qobs, i} - \text{Qcalc, m})^2}} \qquad (4)$$

To evaluate further model simulations in terms of error quantification, another performance criterion was selected to know better the tendency of the model to underestimate or overestimate streamflow. This criterion is the bias error (PBIAS), which varies between $-\infty$ and $+\infty$, with a value of 0 for an unbiased model. Generally, the hydrological model underestimates flows when the value of this criterion is positive, but negative values indicate an overestimation of flows [70]. The descriptive equation for this criterion is written as follows:

$$\text{PBIAS \%} = \frac{\sum_{i=1}^{n}(\text{Qobs, i} - \text{Qcalc, i})}{\sum_{i=1}^{n} \text{Q, obs, i}} * 100 \qquad (5)$$

where $Q_{obs,i}$; $Q_{calc,i}$; and $Q_{obs,m}$ present the observed and simulated flows over a time step and the average of the observed flows, respectively. These functions compare the model simulation on the n-time step with the mean of the observations taken as a reference model.

3. Results

3.1. Model Calibration (GR4J)

The calibration consisted of selecting the set of model parameters known as optimal values that give the best simulation results over the calibrated period. In this study, manual calibration was used to find the best fit between the observed and simulated hydrographs. The split sample method consisted of dividing the simulated period into two equal parts: the first part that is between 1 January 2002 and 31 December 2006 was used for model calibration, while the second part was usable to validate the model. After calibration, relevant results were found and are depicted in Figure 8.
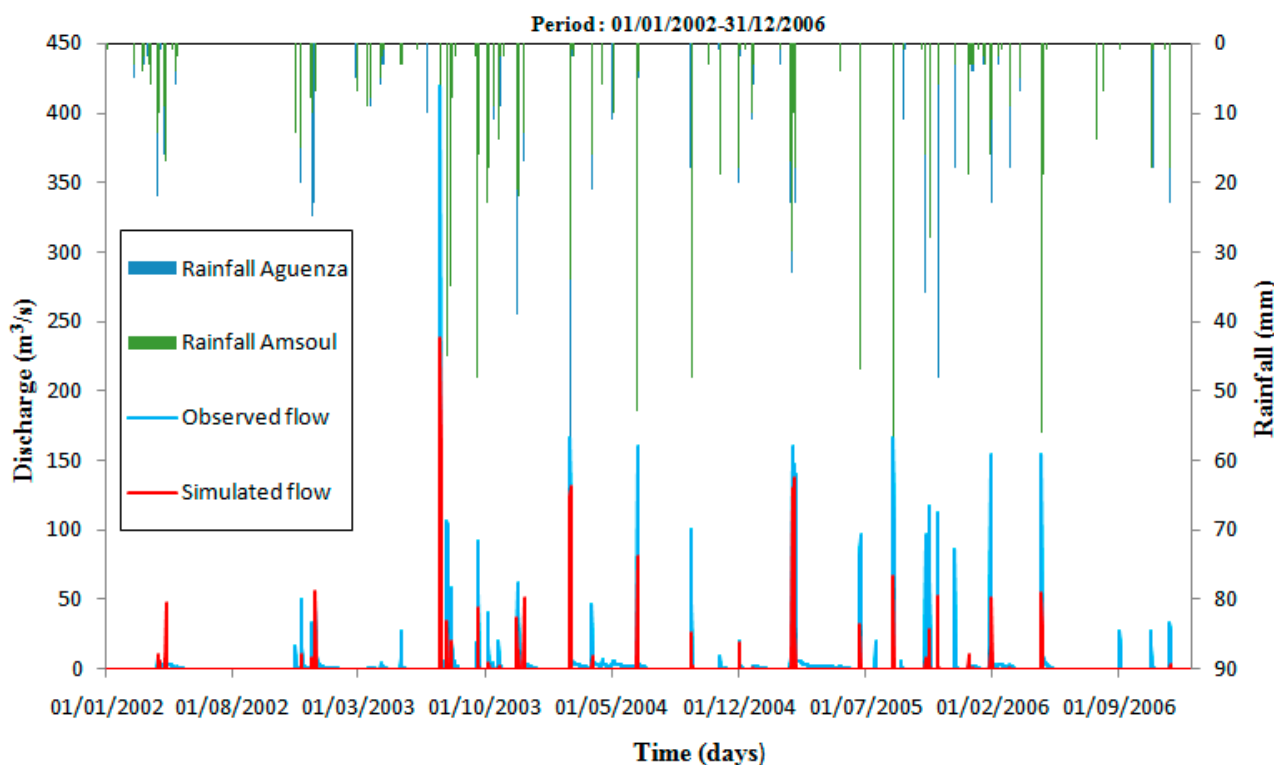
Figure 8. Illustration of the GR4J model output visualization during the period between 2002 and 2006.

The simulated hydrographs by the GR4J model are in daily time steps. This time step is particularly interesting for the problems of preservation of the aquatic environment: a single day of unmet needs is enough to affect the hydrological cycle [71–73]. By comparing the daily flows (Figure 8), it was observed and simulated that the values are essentially close for days with low flows, which indicates a good restitution of baseflow. Overall, the calibrated model has the following advantages/disadvantages:

- Peak flows are underestimated;
- The low flow is correctly simulated;
- The modeled values are close to the observed values.

The daily variability of the flows is remarkable in the simulation periods. This variability of the daily flows is expressed in the model by the level of the production tank (X_1) and the capacity of the routing tank (X_3). Our model has four parameters not directly measured in the field. The optimal values of calibrated parameters obtained for the GR4J model are depicted in Table 1. From the analysis of these values, it is can be noticed that they are in the same range of variation as those obtained by Perrin et al. [51].

Table 1. Optimal values of the model parameters (GR4J).

Procedure	Simulation Period	Parameters	Optimal Values
Calibration	1 January 2002–31 December 2006	X1	4.3
		X2	0.6
		X3	1.7
		X4	−0.7
Validation	1 January 2007–31 December 2011	X1	4.3
		X2	0.6
		X3	1.7
		X4	−0.7

A sensitivity analysis was adopted in this study that consisted of identifying the most sensitive parameters that influence the overall shape of the simulated hydrograph and produce significant changes in model performance to isolate the effect of certain parameters [74]. Default parameter values are changed within the ranges of these parameters to determine which parameters influence the final results [75]. In terms of the GR4J model parameter sensitivity, the most sensitive parameters were found to be the capacity of the production reservoir (X1) and the routing reservoir (X3). Therefore, by focusing on these two parameters, the best set was finally reached for the NSE, RSR, PBIAS, and R^2 performance criteria (Table 2). Consequently, this shows that the quality of our simulation is satisfactory (NSE value of about 0.57).

Table 2. Performance comparison of the results of two hydrological models used (GR4J and ATHYS).

Procedure	Simulation Period	GR4J Model			ATHYS Model		
		Performance Criteria	Values	Evaluation	Performance Criteria	Values	Evaluation
Calibration	1 January 2002–31 December 2006	NSE	0.57	Satisfactory *	NSE	0.65	Good *
		RSR	0.65	Satisfactory	RSR	0.59	Good
		PBIAS	67.8	No satisfactory *	PBIAS	22.6	Satisfactory *
		R²	0.63	Good	R²	0.62	Good
Validation	1 January 2007–31 December 2011	NSE	0.52	Satisfactory *	NSE	0.58	Satisfactory *
		RSR	0.69	Satisfactory	RSR	0.65	Satisfactory
		PBIAS	10.5	Good *	PBIAS	1.6	Very good *
		R²	0.62	Good	R²	0.61	Good

Note: * Noticeable improvement when using a spatially distributed modeling approach.

3.2. Validation of the Model (GR4J)

Model validation is a necessary step to perform efficient hydrological modeling. In this study, the optimal values were used to control the robustness of the GR4J model in the studied context. More precisely, the second sub-period, which was not used in the

calibration phase, was retained for model validation or verification (between 1 January 2007 and 31 December 2011). The analysis of our resulting hydrograph (Figure 9) shows that the applied model is close to the one that simulates the observed hydrograph, especially during low-flow periods.
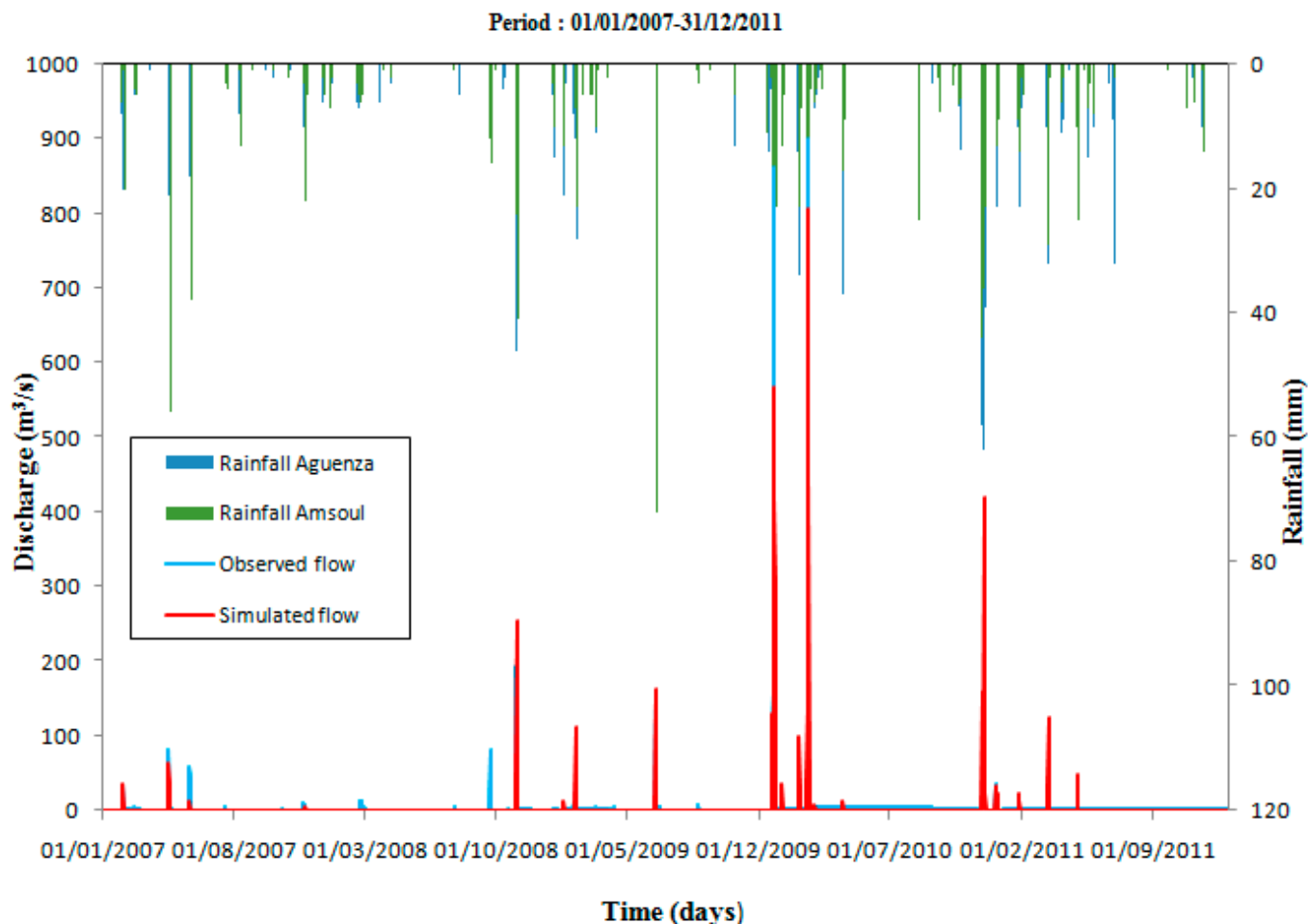
Figure 9. Illustration of the GR4J model output visualization during the period used for validation"2007–2011".

Based on the performance criteria of NSE, RSR, and R^2 presented in Table 2, the results of the rainfall-runoff modeling using the GR4J model during the validation period can be considered satisfactory. However, the PBIAS criterion analysis shows that the model tends to underestimate the flows, with a positive value of +10.5. This indicates that while the model performs well in terms of overall accuracy, there may be some bias in the predictions. Overall, the application of the GR4J model for rainfall-runoff modeling in the study area is satisfactory, which is mainly justified by the agreement between observed and simulated flows as well as the performance criteria values mentioned in Table 2.

3.3. Calibration of the Model (ATHYS)

The ATHYS modeling platform is used to simulate the flows from 1 January 2002 to 31 December 2006 with calibration by computing the streamflow at the Aguenza outlet. Figure 10 presents the results of the calibration of a distributed model over the considered period.

Based on these results, there is good agreement between observations and simulations. Moreover, our findings indicate that the SCS-LR model underestimates the peak flows during the considered period.

Figure 10. Graphical illustration of the ATHYS model output over the five years (2002–2006) used for calibration.

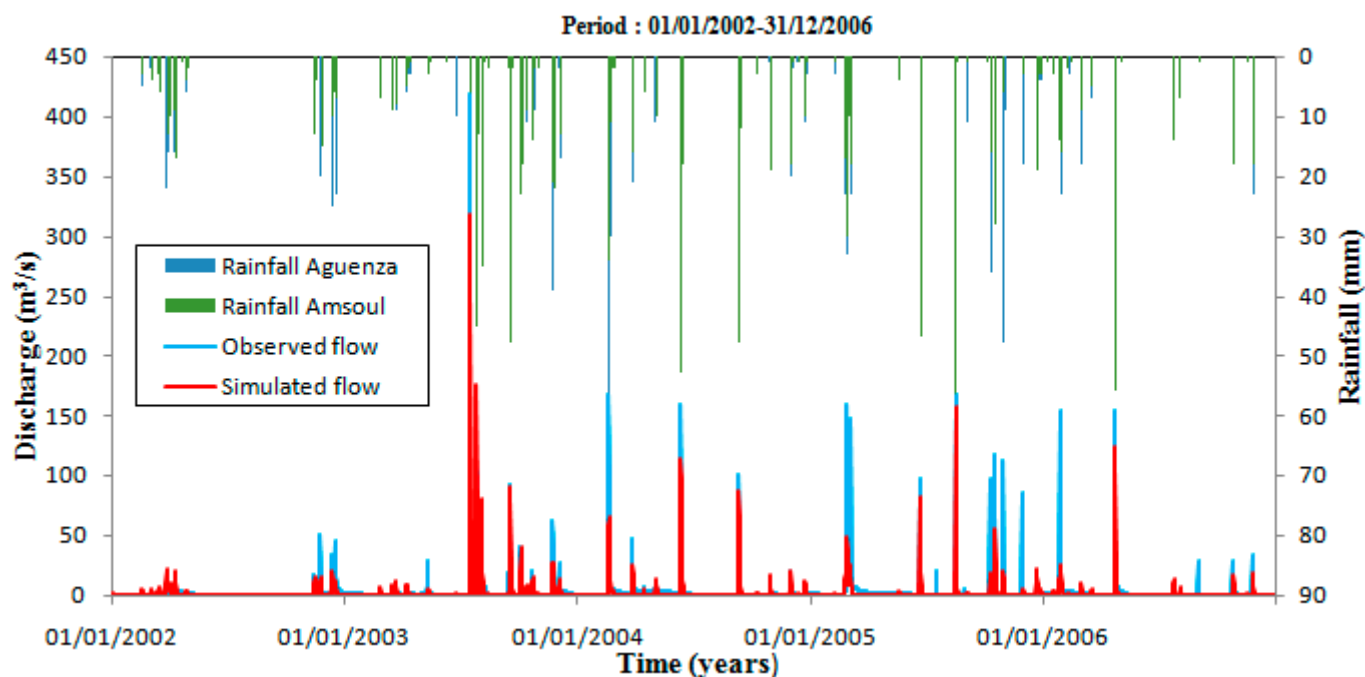The analysis of the resulting parameters (Table 3), which give less difference between observed and modeled flows, shows that these parameters are generally realistic in the study area. The S calibrated value (S = 110 mm) is similar to the S values obtained by Laganier et al. [76], who found a similar range of variation in the Anduze basin with a rural dominance.

Table 3. Optimal parameter values of the ATHYS model.

Procedure	Simulation Period	Parameters				
		S	W	Ds	V_0	k_0
Calibration	1 January 2002–31 December 2006	110	0.2	1.1	3	0.7
Validation	1 January 2007–31 December 2011	110	0.2	1.1	3	0.7

The objective functions used to evaluate this study are successively the NSE, RSR, R^2, and PBIAS criteria. Table 2 shows that the values of NSE and R^2 criteria are successively 0.65 and 0.62. These values mean that the calibration is good according to the classification of Moriasi et al. [68]. Moreover, the value of the RSR error is low (RSR = 0.59), which confirms that our simulation is very efficient. However, the value of the PBIAS is positive, which indicates that our model tends to underestimate flows as illustrated in Figure 10.

3.4. Validation of the Model (ATHYS)

The ATHYS platform was used to validate the model in the Aguenza watershed over the period going from 1 January 2007 to 31 December 2011. By comparing the simulated and observed streamflow (Figure 11), it can be seen that they are in perfect concordance during the summer period. The description of the calibrated model allows concluding that:

- The low-flow period is reproduced well by the model;
- The two large peak flows ((24 December 2009; Q max observed = 864 m^3/s) and (18 February 2010; Q max observed = 902 m^3/s)) are underestimated by the model ((24 December 2009; Q max simulated = 392 m^3/s) and (18 February 2010; Q max simulated = 516 m^3/s)), while the other peaks are correctly restituted by this model.
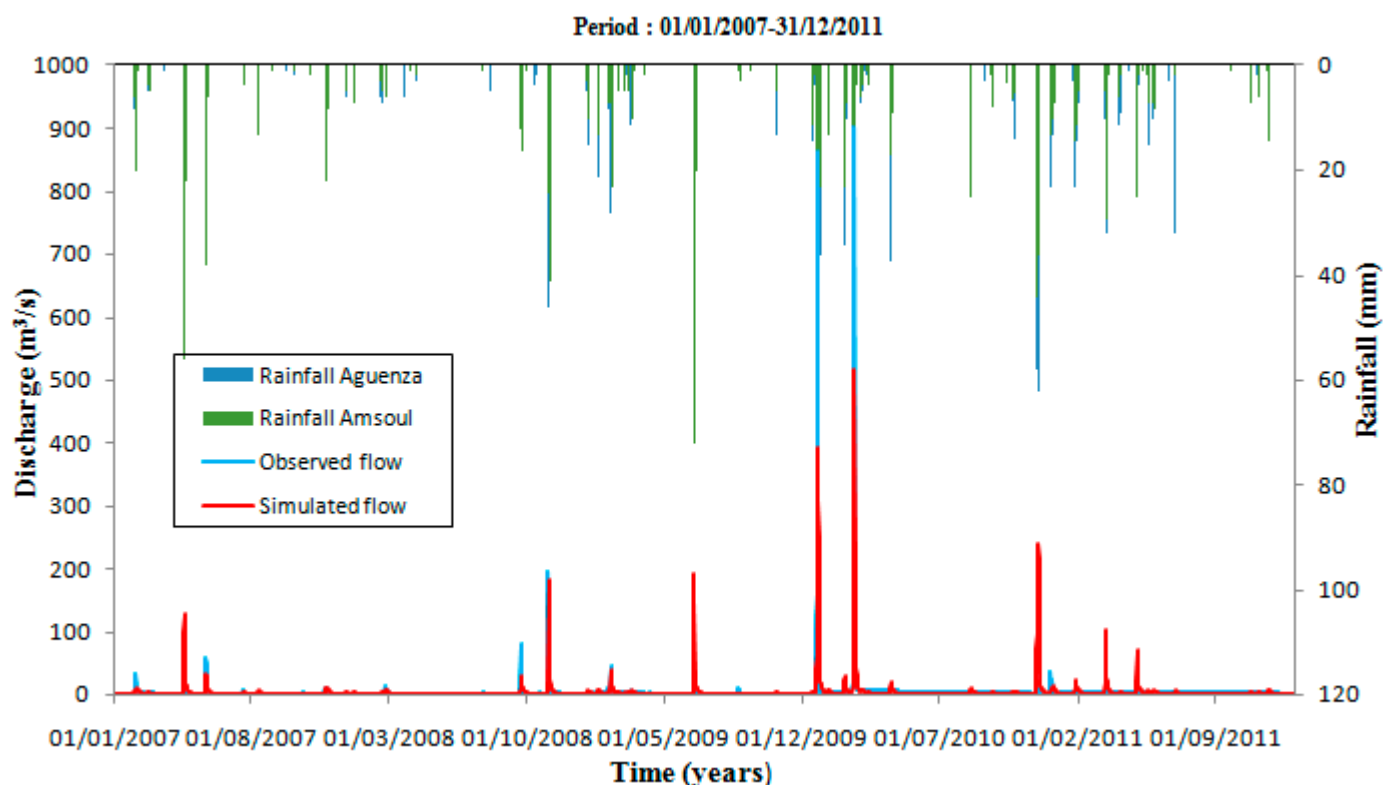
Figure 11. Graphical illustration of the ATHYS model output during the validation period (2007–2011).

To validate the model in this study, the parameter values obtained during the calibration step were used (Table 2) to properly test the ability of the ATHYS model to reproduce other data sets at the Aguenza outlet without changing any of these parameters. Table 2 shows the performance criteria resulting from the validation phase. These parameters give a small difference between the general appearance of the observed and modeled hydrographs. According to the table below, the RSR criterion has a value of 0.65, and the values of NSE and R^2 are higher than 0.5, which means that the quality of performance is satisfactory based on Moriasi et al. [68]. Moreover, the value of the criterion PBIAS (+1.6) indicates a weak underestimation of the flows by the discretized model (ATHYS) in comparison with that obtained by the lumped model ($PBIAS_{GR4J}$ = +10.5), which makes it possible to say that the discretized model succeeded well in reproducing the regime of flow at the Aguenza outlet. This finding allows concluding that taking into account the spatial variation of precipitation and topography can clearly improve the model performance and consequently the streamflow simulations in the Aguenza watershed.

3.5. Event-Based Simulations (ATHYS)

Insufficient knowledge of hydrological events can cause economic and sometimes human damage [22]. Therefore, in this context, it is easy to understand the need for an adequate estimation of these extreme hydrological events. The event-based modeling consisted of reproducing the flood hydrograph, mainly in the parts of flood rise, peak flows, and beginning of the recession until the drying up, all based on the histograms of precipitation observed in the Aguenza and Amsoul rain gauge stations of the studied watershed, to finally reproduce well the simulated flood hydrographs as the model output. The calibration consisted of assigning to the parameters the numerical values, leading to minimizing the difference between the calculated responses and the observed responses. The two most important elements of this procedure are the following:

- Assessment of the quality of the simulations by adopting a performance measurement;

- The method of modifying the parameters if the concordance between the observed and simulated values is insufficient.

The ATHYS platform was used also to simulate 10 important rainfall events available between 1984 and 2014 at the Aguenza stations, with maximum rainfall intensity at an hourly time step ranging from 2.90 to 13.20 mm·h^{-1} and a peak flow ranging from 50 m^3·s^{-1} to 425 m^3·s^{-1}. By adopting the split sample method, the first five events were used to calibrate the model, while the remaining events were used to validate the model. These events are listed in increasing chronological order in Table 4.

Table 4. Classification of events according to applied modeling procedure.

N° Event	Start Date/End Date	Maximum Rainfall Intensity (mm·h^{-1}) Time Step = 60 min	Procedure
1	4 November 1984 15:00–12 November 1984 13:00	9.25	Calibration
2	15 October 1988 01:00–20 October 1988 22:00	2.90	Calibration
3	9 November 1988 09:00–13 November 1988 23:00	6.25	Calibration
4	17 February 1991 00:00–23 February 1991 00:00	4.70	Calibration
5	10 January 1996 01:00–24 January 1996 04:00	13.20	Calibration
6	1 January 1997 00:00–8 January 1997 00:00	10.20	Validation
7	1 February 1998 00:00–7 February 1998 00:00	4.90	Validation
8	6 December 1999 10:00–11 December 1999 15:00	3.90	Validation
9	21 December 2000 14:00–23 December 2000 13:00	8.65	Validation
10	28 November 2014 04:00–28 November 2014 22:00	9.30	Validation

Climate information is collected periodically at each station. This information needs to be spatialized to be extended to the entire watershed area. The Thiessen polygon method was used to spatialize the precipitation provided by Aguenza and Amsoul rain gauge stations by defining the area of influence of each station. The smallest time step available for flood episodes is 60 min. In this part of the study, the SCS model was chosen as a production function, and lag and route (LR) was chosen as a transfer function.

Upon comparison of the hourly discharge values, as shown in Figure 12, it can be observed that the observed and simulated values are closely aligned, particularly during periods of low flow. The calibrated model has the following strengths and weaknesses: (i) the model tends to underestimate peak flows; (ii) however, overall, the simulated results are highly comparable to the observed data.

Calibration consisted of adjusting the numerical values assigned to the model parameters to reproduce the observed response. In this study, a manual procedure was used by sensitivity analysis mainly for the three production function parameters (S, w, and ds) and then for the transfer function parameters (V_0 and K_0). The parameters of the coupled SCS-LR model were manually modified by the trial and error technique to reduce the difference between the observed and calculated flows. The influence on the overall appearance of the simulated hydrograph differs from one parameter to another, which reflects the importance of performing a sensitivity analysis to determine the most and least influential parameters on the model results and automatically on the values of the objective functions chosen to evaluate these results. From the sensitivity analysis performed, the following can be concluded:

- The change in the S-parameter values (SCS) has a strong influence on the peak flow;
- The decrease of the hydrogram explained by the emptying time is generally influenced by the parameter "ds", which allows seeing a better appearance between the simulated and the observed in terms of drying.

The parameters that have less influence on the general appearance of the hydrograph are fixed, essentially for the transfer function, namely the diffusion coefficient (K_0), and for the production function the parameter (ω), which represents the emptying fraction that participates in runoff and generally varies slightly from one event to another. Previous studies in Morocco have shown that similar parameters have a significant impact on the flow [20,22]. Table 5 shows that the variability of the parameters S, ds, and velocity

(V_0) transfer parameter is very large, which means their remarkable influences on the hydrograph and the other parameters have very low values.
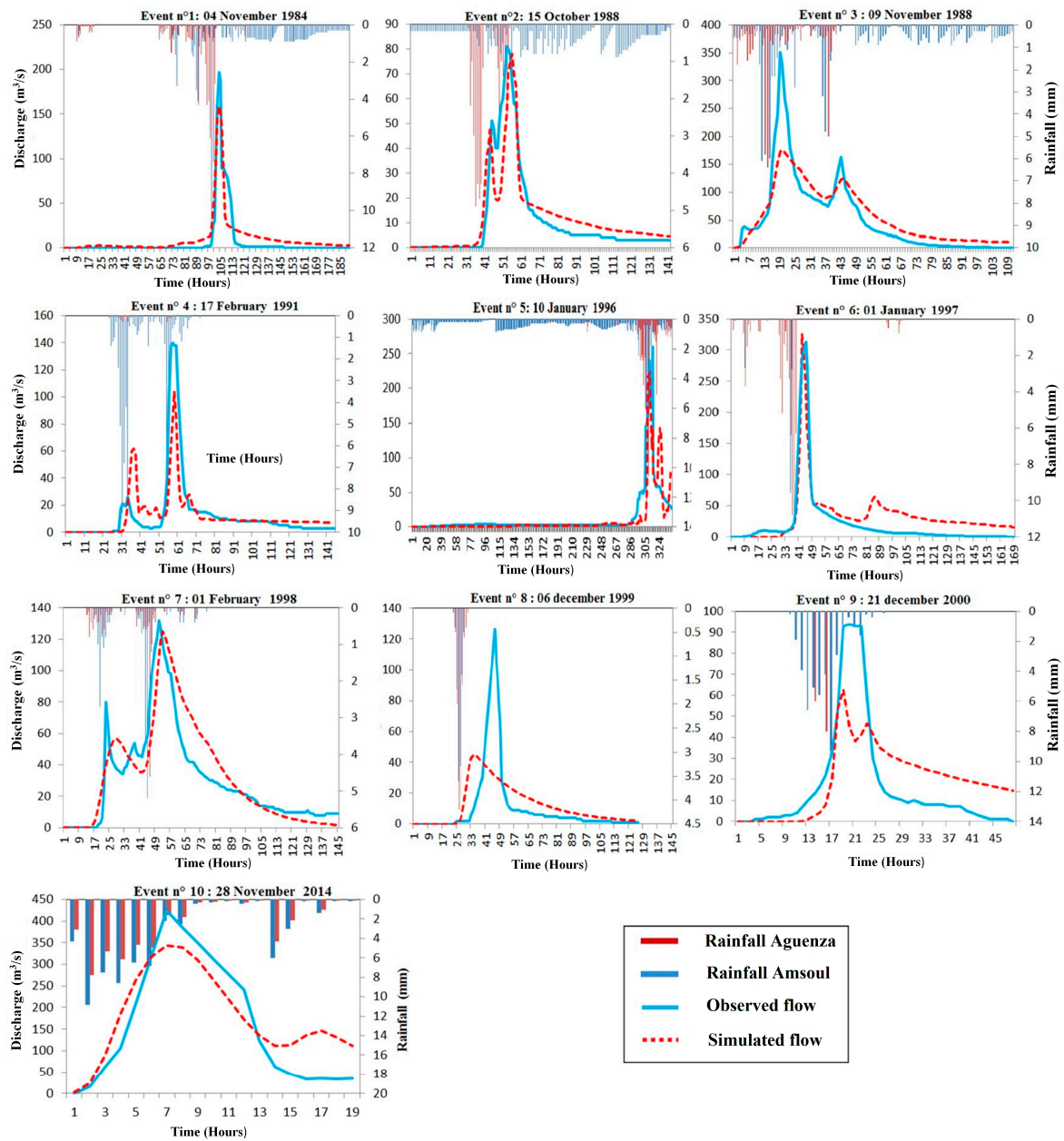
Figure 12. Simulation results for the ten events used for model calibration (events 1, 2, 3, 4, and 5) and validation (events 6, 7, 8, 9, and 10) (time step = 60min).

Table 5. The parameters resulting from events calibration (ATHYS).

N° Event	Episodes	Parameters				
		S	W	Ds	V_0	K_0
1	4 November 1984	100	0.1	1	2.9	0.7
2	15 October 1988	90	0.1	0.6	3	0.7
3	9 November 1988	120	0.5	1.8	3.4	0.7
4	17 February 1991	100	0.3	0.6	2.4	0.7
5	10 January 1996	120	0.1	0.3	2.6	0.7
	Average	106	0.2	0.9	2.9	0.7

Evaluation of the Model

After calibration and validation of the model, it was necessary to evaluate its quality. Generally, the evaluation of the quality of a simulation can sometimes be used as an objective function or performance measure during model calibration and validation. Table 6 determines the quality of the modeling based on the values of the performance criteria used in this study. This table also shows the variation in performance criteria from one event to another. According to Table 6, the average NSE, PBIAS, R^2, and RSR values of the events selected for calibration were 0.76, −7.57, 0.74, and 0.48, respectively.

Table 6. Statistical analysis of calibration and validation events by calculating some performance criteria.

N° Event	Episode	Criteria				Performance Evaluation
		PBIAS	RSR	R^2	NSE	
1	4 November 1984	−42.81	0.41	0.82	0.83	Very good
2	15 October 1988	−9.35	0.42	0.79	0.82	Very good
3	9 November 1988	−8.07	0.46	0.69	0.78	Very good
4	17 February 1991	4.71	0.62	0.65	0.62	Satisfactory
5	10 January 1996	17.68	0.51	0.75	0.74	Good
	Average	−7.57	0.48	0.74	0.76	Very good
6	1 January 1997	36.62	0.53	0.86	0.72	Good
7	1 February 1998	−8.55	0.48	0.81	0.77	Very good
8	6 December 1999	−11.06	0.80	0.37	0.36	No satisfactory
9	21 December 2000	−14.37	0.71	0.52	0.50	Satisfactory
10	28 November 2014	−11.21	0.45	0.86	0.80	Very good
	Average	−1.71	0.59	0.68	0.63	Satisfactory

However, the quality of the simulation during the calibration phase is satisfactory for only one event, while for the others, the quality of the simulation varies from good to very good. This indicates the very high capacity of the ATHYS platform to reproduce flood events in the semi-arid context. This finding must be confirmed during the validation phase. The latter was developed in this study using the average values of the parameters retained during the calibration. The results obtained after using the values of the parameters listed in Table 5 give the hydrographs presented in Figure 12. The final results obtained in the validation phase also confirm the applicability of the spatially distributed SCS-LR model, with mean values of NSE, PBIAS, R^2, and RSR of 0.63, −1.71, 0.68, and 0.59, respectively.

Table 7 presents a detailed analysis of the hydrographs resulting from the calibration and validation processes, as obtained from the output files. The table provides an in-depth understanding of the hydrographs illustrated above. For the validation phase, recent events were selected to validate the model; this choice was made to ensure that the model could accurately simulate the most recent events. This is important to ensure that the model can accurately predict future events and support the management and conservation of water resources in the area.

Table 7 presents the characteristics of the observed and simulated hydrographs used during the calibration and validation procedures. Further analysis of these indicates and confirms the tendency of the coupled model (SCS-LR) to underestimate flows (observed peak flows are higher than modeled for all events). Similarly, the runoff volumes are logical and largely reflect the actual flow system in the study area. Furthermore, note that the rise times in the simulated hydrographs are higher than those of the observed hydrographs.

Table 7. Characteristics extracted by hydrographs after model calibration and validation.

		Characteristics							
		Observed Hydrograph				Simulated Hydrograph			
N° Event	Episodes	Peak Flow (m^3/s)	Runoff Volume (km^3)	Rise Time (mn)	Basic Time (h)	Peak Flow (m^3/s)	Runoff Volume (km^3)	Rise Time (mn)	Basic Time (h)
1	4 November 1984	197	4824	480	21	159	6136	3180	41
2	15 October 1988	81	4996	660	28	77.9	4944	3060	26
3	9 November 1988	351	21,081	1080	52	176	20,673	1920	54
4	17 February 1991	140	6067	720	39	104	4822	2040	41
5	10 January 1996	261	4114	1560	47	223	13,226	10,080	37
6	1 January 1997	326	16,383	1440	21	313	12,656	2100	40
7	1 February 1998	132	13,867	1320	72	125	16,886	1620	78
8	6 December 1999	126	4741	960	30	44.9	5071	720	38
9	21 December 2000	94	2876	840	24	62.7	2238	720	16
10	28 November 2014	425	9869	480	13	343	8421	540	14

4. Discussion

The estimation of streamflow in the data-scarce Aguenza watershed was made using two models with different characteristics: the conceptual and lumped model GR4J, which does not take into consideration the spatial variability of the hydrological processes, and the spatially distributed model ATHYS, which estimates the water level on each mesh by taking into account the spatial organization of various factors influencing streamflow generation.

The results obtained after the implementation of the two hydrological models mentioned above in the Aguenza watershed confirm that the inclusion of spatial information improves the modeling results, particularly for the calibration period, where the use of ATHYS led to an improvement of 8%, 6%, and 45.2% in the values of NSE, RSR, and PBIAS, respectively, compared to GR4J. Additionally, during the validation process, the use of the spatially distributed model ATHYS resulted in a remarkable increase in model performance, with NSE values improving by 6% and errors estimated by the RSR and PBIAS criteria minimized by 4% and 8.9%. These findings demonstrate the benefit of using a distributed approach in the estimation of flows in the studied watershed. The validation results obtained using the two models on the Aguenza watershed are satisfactory (NSE > 0.5), indicating that these models are suitable for use in semi-arid areas, specifically in the southwest of Morocco, where the Aguenza watershed is located.

The GR4J model and the coupled SCS-LR model tend to underestimate flows in the studied watershed. In general, the underestimation or overestimation of peak flows is closely related to land use, soil type, and saturation, especially in arid and semi-arid areas [11,20,21,77–80]. In these environments, the rainfall–runoff transformation primarily depends on the soil saturation condition where, for example, during the dry period, the first rain events seep through the previous layer and do not transform into surface runoff. It should also be noted that the most recent layer of the geology of the Aguenza watershed is formed mainly by dolomitic limestones and fine sandstones, forming the most erosion-resistant soils [81], as these types of soils allow better infiltration of surface water and subsequently influence the underestimation of peak flows in karstic basins [77,82,83]; this is confirmed by the very important value of the parameter of a total capacity of the ground reservoir (S = 110 mm); therefore, a great quantity of precipitation is lost by infiltration, causing the underestimation of the peaks of flow during the hydrological modeling of the basins of karstic and rural nature.

Nevertheless, this ATHYS model has a very important advantage because it allows the good reproduction of low flows, which have a very important impact on the hydrological cycle, and it also allows the consideration of the water exchanges between the surface and the underground, which reduces greatly the significant underestimation of the peak flows during hydrological modeling of the karst areas.

Event-based models have several advantages over continuous models and are often preferred for real-time and operational applications [56]. They require only event-scale data and avoid the use of full-time series, and they consider only event-scale flood processes. In this study, event-based modeling is elaborated to allow the simulation of the rainfall–runoff

relationship to simulate the hydrologic behavior of the Aguenza watershed for a specific operating mode. In general, flood events are used without considering the specification of the history of previous conditions.

The results obtained for 70% of the events selected for calibration and validation have a quality between good and very good, which shows the applicability of the coupled model SCS-LR in the Aguenza watershed. It should be noted that the underestimation of point flows in all events is mainly due to the karstic and rural nature of the studied watershed [81]. Nevertheless, the rise time in the simulated hydrographs is higher than those of the observed hydrographs, which is mainly due to the difficulties encountered in accessing data related to the hydrodynamic properties of the soils; this condition and the simplicity and applicability of the empirical SCS model in semi-arid areas [20,84,85] were among the main conditions for the implementation of the SCS model that does not take into consideration the state of soil moisture before each rainfall event and subsequent influences on the simulation of the rise times.

Finally, it is important to note the importance of this study regarding knowing the evolution of floods and the resulting volumes after a rain event for better management of water resources in areas with a semi-arid climate that is characterized by a non-linear relationship between the volumes of water runoff and rainfall [85]. The reservoirs of these areas strongly influence the amount of water runoff, especially after a long period of absence or low precipitation in semi-arid basins of karst nature such as the Aguenza Basin which is the subject of this study, and all these factors generally make the simulation of flows more and more complicated in watersheds with arid and semi-arid climates [86–89].

5. Conclusions

This work focused on rainfall-flow modeling using two different models: one the global "GR4J" and the other the discretized "ATHYS". The first phase aimed to study the influence of the spatialization of the watersheds on the modeling results through the use of two hydrological models with different characteristics, and the second phase consisted of using the ATHYS model to simulate the flows by applying the event-based approach and to study the main floods that occurred between 1984 and 2014 in the Aguenza watershed.

The obtained results from the comparative study of lumped and distributed models show the importance of taking into account the hydrological processes since, after the use of the discretized model "ATHYS", remarkable improvements were observed in the general aspect of the resulting hydrographs. This improvement was also confirmed based on the performance criteria; as an example, the value of NSE during the calibration process increased successively by 8%, and the errors were minimized by 45.2% according to the PBIAS criterion when applying the SCS-LR model instead of the GR4J model. In this context, it is necessary to understand the importance of taking into account the hydrological processes during the modeling to obtain realistic results close to the reality of the watersheds. The validation results of the two hydrological models are satisfactory (average of NSE = 0.55), which confirms their applicability in the semi-arid context.

In this study, an event-mode model was also developed to allow the simulation of the rainfall–runoff relationship to simulate the hydrological behavior of the Aguenza watershed for a specific operating mode. In general, flood events are used without considering the specification of the history of previous conditions. The results obtained by applying the ATHYS model in event mode are interesting and give appreciable results, namely that the values of the NSE criterion obtained for the calibration procedure vary between 0.60 and 0.83 as the maximum value. During the validation procedure, although the observed contrast in the quality of the results is remarkable, the average value of the NSE (average NSE = 0.60) shows that the validation was well done, and this confirms the first results obtained by the ATHYS and GR4J models in continuous mode.

By comparing and analyzing the results and simulations, decision-makers can understand the hydrological behavior in the considered watershed to better specify the limits of this study, to allow an evaluation of the availability and/or access to data to find much more

relevant simulation results in the future, and also to increase the relevance and applicability of other hydrological models with different characteristics.

Author Contributions: Conceptualization, A.B. and I.B.; methodology, M.A. (Mourad Aqnouy) and I.H.; software, A.B.; validation, M.A. (Mourad Aqnouy), K.A., L.B., J.E.S.E.M. and M.A. (Mohamed Abioui); formal analysis, A.B., I.B. and K.A.; investigation, K.E.-n., Y.E.Y. and A.K.; resources, A.B.; data curation, A.B., A.K. and I.H.; writing—original draft preparation, A.B., I.B. and L.B.; writing—review and editing, M.A. (Mourad Aqnouy), K.A., T.A.-A., J.E.S.E.M. and M.A. (Mohamed Abioui); visualization, M.A. (Mourad Aqnouy), K.E.-n., Y.E.Y., A.K. and M.A. (Mohamed Abioui); supervision, L.B.; project administration, M.A. (Mohamed Abioui); funding acquisition, K.A. All authors have read and agreed to the published version of the manuscript.

Informed Consent Statement: Not applicable.

Data Availability Statement: The data that support the findings of this study are available from the corresponding authors upon reasonable request.

Conflicts of Interest: The authors declare no conflict of interest.

References

1. Shen, Y.; Chen, Y. Global Perspective on Hydrology, Water Balance, and Water Resources Management in Arid Basins. *Hydrol. Processes* **2010**, *24*, 129–135. [CrossRef]
2. Deng, L.; Guo, S.; Yin, J.; Zeng, Y.; Chen, K. Multi-Objective Optimization of Water Resources Allocation in Han River Basin (China) Integrating Efficiency, Equity and Sustainability. *Sci. Rep.* **2022**, *12*, 798. [CrossRef] [PubMed]
3. Bouizrou, I.; Aqnouy, M.; Bouadila, A. Spatio-Temporal Analysis of Trends and Variability in Precipitation across Morocco: Comparative Analysis of Recent and Old Non-Parametric Methods. *J. Afr. Earth Sci.* **2022**, *196*, 104691. [CrossRef]
4. Gunkel, A.; Shadeed, S.; Hartmann, A.; Wagener, T.; Lange, J. Model Signatures and Aridity Indices Enhance the Accuracy of Water Balance Estimations in a Data-Scarce Eastern Mediterranean Catchment. *J. Hydrol. Reg. Stud.* **2015**, *4*, 487–501. [CrossRef]
5. Ahmed, M.; Aqnouy, M.; Stitou El Messari, J. Sustainability of Morocco's Groundwater Resources in Response to Natural and Anthropogenic Forces. *J. Hydrol.* **2021**, *603*, 126866. [CrossRef]
6. Morote, Á.-F.; Olcina, J.; Hernández, M. The Use of Non-Conventional Water Resources as a Means of Adaptation to Drought and Climate Change in Semi-Arid Regions: South-Eastern Spain. *Water* **2019**, *11*, 93. [CrossRef]
7. El Yousfi, Y.; Himi, M.; El Ouarghi, H.; Aqnouy, M.; Benyoussef, S.; Gueddari, H.; Ait Hmeid, H.; Alitane, A.; Chaibi, M.; Zahid, M.; et al. Assessment and Prediction of the Water Quality Index for the Groundwater of the Ghiss-Nekkor (Al Hoceima, Northeastern Morocco). *Sustainability* **2023**, *15*, 402. [CrossRef]
8. El Yousfi, Y.; Himi, M.; El Ouarghi, H.; Elgettafi, M.; Benyoussef, S.; Gueddari, H.; Aqnouy, M.; Salhi, A.; Alitane, A. Hydrogeochemical and Statistical Approach to Characterize Groundwater Salinity in the Ghiss-Nekkor Coastal Aquifers in the Al Hoceima Province, Morocco. *Groundw. Sustain. Dev.* **2022**, *19*, 100818. [CrossRef]
9. Jarlan, J.; Khabba, S.; Er-Raki, S.; Le Page, M.; Hanich, H.; Fakir, Y.; Merlin, O.; Mangiarotti, S.; Gascoin, S.; Ezzahar, J.; et al. Remote Sensing of Water Resources in Semi-Arid Mediterranean Areas: The Joint International Laboratory TREMA. *Int. J. Remote Sens.* **2015**, *36*, 4879–4917. [CrossRef]
10. Lian, X.; Piao, S.; Chen, A.; Huntingford, C.; Fu, B.; Li, L.Z.X.; Huang, J.; Sheffield, J.; Berg, A.M.; Keenan, T.F.; et al. Multifaceted Characteristics of Dryland Aridity Changes in a Warming World. *Nat. Rev. Earth Environ.* **2021**, *2*, 232–250. [CrossRef]
11. Yu, Q.; Jiang, L.; Wang, Y.; Liu, J. Enhancing Streamflow Simulation Using Hybridized Machine Learning Models in a Semi-Arid Basin of the Chinese Loess Plateau. *J. Hydrol.* **2023**, *617*, 129115. [CrossRef]
12. Payus, C.; Ann Huey, L.; Adnan, F.; Besse Rimba, A.; Mohan, G.; Kumar Chapagain, S.; Roder, G.; Gasparatos, A.; Fukushi, K. Impact of Extreme Drought Climate on Water Security in North Borneo: Case Study of Sabah. *Water* **2020**, *12*, 1135. [CrossRef]
13. De Mello, K.; Taniwaki, R.H.; de Paula, F.R.; Valente, R.A.; Randhir, T.O.; Macedo, D.R.; Leal, C.G.; Rodrigues, C.B.; Hughes, R.M. Multiscale Land Use Impacts on Water Quality: Assessment, Planning, and Future Perspectives in Brazil. *J. Environ. Manag.* **2020**, *270*, 110879. [CrossRef] [PubMed]
14. Alpert, P.; Ben-Gai, T.; Baharad, A.; Benjamini, Y.; Yekutieli, D.; Colacino, M.; Diodato, L.; Ramis, C.; Homar, V.; Romero, R.; et al. The Paradoxical Increase of Mediterranean Extreme Daily Rainfall in Spite of Decrease in Total Values. *Geophys. Res. Lett.* **2002**, *29*, 31-1–31-4. [CrossRef]

15. Alpert, P.; Osetinsky, I.; Ziv, B.; Shafir, H. Semi-Objective Classification for Daily Synoptic Systems: Application to the Eastern Mediterranean Climate Change. *Int. J. Climatol.* **2004**, *24*, 1001–1011. [CrossRef]

16. Abdrabo, K.I.; Kantosh, S.A.; Saber, M.; Sumi, T.; Elleithy, D.; Habiba, O.M.; Alboshy, B. The Role of Urban Planning and Landscape Tools Concerning Flash Flood Risk Reduction within Arid and Semiarid Regions. In *Wadi Flash Floods*; Sumi, T., Kantoush, S.A., Saber, M., Eds.; Springer: Singapore, 2022; pp. 283–316. [CrossRef]

17. Kastridis, A.; Stathis, D. Evaluation of Hydrological and Hydraulic Models Applied in Typical Mediterranean Ungauged Watersheds Using Post-Flash-Flood Measurements. *Hydrology* **2020**, *7*, 12. [CrossRef]

18. Papaioannou, G.; Efstratiadis, A.; Vasiliades, L.; Loukas, A.; Papalexiou, S.M.; Koukouvinos, A.; Tsoukalas, I.; Kossieris, P. An Operational Method for Flood Directive Implementation in Ungauged Urban Areas. *Hydrology* **2018**, *5*, 24. [CrossRef]

19. Aqnouy, M.; Stitou El Messari, J.E.; Bouadila, A.; Morabbi, A.; Benaabidate, L.; Al-Djazouli, M.O. Modeling of Continuous and Extreme Hydrological Processes Using Spatially Distributed Models Mercedes, Vicair and Vishyr in a Mediterranean Watershed. *Ecol. Eng. Environ. Technol.* **2021**, *22*, 9–23. [CrossRef]

20. Bouizrou, I.; Chahinian, N.; Perrin, J.L.; Müller, R.; Rais, N. Network Representation in Hydrological Modelling on Urban Catchments in Data-Scarce Contexts: A Case Study on the Oued Fez Catchment (Morocco). *J. Hydrol. Reg. Stud.* **2021**, *34*, 100800. [CrossRef]

21. Bouadila, A.; Benaabidate, L.; Bouizrou, I.; Aqnouy, M. Implementation of Distributed Hydrological Modeling in a Semi-Arid Mediterranean Catchment Azzaba, Morocco. *J. Ecol. Eng.* **2019**, *20*, 236–254. [CrossRef]

22. Aqnouy, M.; Ahmed, M.; Ayele, G.T.; Bouizrou, I.; Bouadila, A.; Stitou El Messari, J.E. Comparison of Hydrological Platforms in Assessing Rainfall-Runoff Behavior in a Mediterranean Watershed of Northern Morocco. *Water* **2023**, *15*, 447. [CrossRef]

23. El Yousfi, Y.; Himi, M.; El Ouarghi, H.; Aqnouy, M.; Benyoussef, S.; Gueddari, H.; Ait Hmeid, H.; Alitane, A.; Chahban, M.; Bourdan, S.; et al. GIS preprocessing for rainfall-runoff modeling using HEC-HMS in Nekkor watershed (Al-Hoceima, Northern Morocco). *E3S Web Conf.* **2023**, *364*, 01005. [CrossRef]

24. Wang, W.; Lu, H.; Yang, D.; Sothea, K.; Jiao, Y.; Gao, B.; Peng, X.; Pang, Z. Modelling Hydrologic Processes in the Mekong River Basin Using a Distributed Model Driven by Satellite Precipitation and Rain Gauge Observations. *PLoS ONE* **2016**, *11*, e0152229. [CrossRef] [PubMed]

25. Hassan, S.M.T.; Lubczynski, M.W.; Niswonger, R.G.; Su, Z. Surface-Groundwater Interactions in Hard Rocks in Sardon Catchment of Western Spain: An Integrated Modeling Approach. *J. Hydrol.* **2014**, *517*, 390–410. [CrossRef]

26. Ikirri, M.; Faik, F.; Echogdali, F.Z.; Antunes, I.M.H.R.; Abioui, M.; Abdelrahman, K.; Fnais, M.S.; Wanaim, A.; Id-Belqas, M.; Boutaleb, S.; et al. Flood Hazard Index Application in Arid Catchments: Case of the Taguenit Wadi Watershed, Lakhssas, Morocco. *Land* **2022**, *11*, 1178. [CrossRef]

27. Thornes, J.; López-bermúdez, F.; Woodward, J. Hydrology, River Regimes, and Sediment Yield. In *The Physical Geography of the Mediterranean*; Woodward, J.C., Ed.; Oxford University Press: Oxford, UK, 2009; pp. 229–253.

28. Manzoor, Z.; Ehsan, M.; Khan, M.B.; Manzoor, A.; Akhter, M.M.; Sohail, M.T.; Hussain, A.; Abu-Alam, T.; Abioui, M. Floods and flood management and its socio-economic impact on Pakistan: A review of the empirical literature. *Front. Environ. Sci.* **2022**, *10*, 1021862. [CrossRef]

29. Carey, M. Living and Dying with Glaciers: People's Historical Vulnerability to Avalanches and Outburst Floods in Peru. *Glob. Planet. Chang.* **2005**, *47*, 122–134. [CrossRef]

30. Ait Haddou, M.; Wanaim, A.; Ikirri, M.; Aydda, A.; Bouchriti, Y.; Abioui, M.; Kabbachi, B. Digital Elevation Model-Derived Morphometric Indices for Physical Characterization of the Issen Basin (Western High Atlas of Morocco). *Ecol. Eng. Environ. Technol.* **2022**, *23*, 285–298. [CrossRef]

31. Echogdali, F.Z.; Boutaleb, S.; Kpan, R.B.; Ouchchen, M.; Bendarma, A.; El Ayady, H.; Abdelrahman, K.; Fnais, M.S.; Sajinkumar, K.S.; Abioui, M. Application of Fuzzy Logic and Fractal Modeling Approach for Groundwater Potential Mapping in Semi-Arid Akka Basin, Southeast Morocco. *Sustainability* **2022**, *14*, 10205. [CrossRef]

32. Bouadila, A.; Tzoraki, O.; Benaabidate, L. Hydrological Modeling of Three Rivers under Mediterranean Climate in Chile, Greece, and Morocco: Study of High Flow Trends by Indicator Calculation. *Arab. J. Geosci.* **2020**, *13*, 1057. [CrossRef]

33. Tramblay, Y.; Bouaicha, R.; Brocca, L.; Dorigo, W.; Bouvier, C.; Camici, S.; Servat, E. Estimation of Antecedent Wetness Conditions for Flood Modelling in Northern Morocco. *Hydrol. Earth Syst. Sci.* **2012**, *16*, 4375–4386. [CrossRef]

34. Aqnouy, M.; Stitou El Messari, J.E.; Hillal, I.; Bouadila, A.; Moreno-Navarro, J.G.; Bounab, L.; Aoulad Mansour, M.R. Assessment of the SWAT Model and the Parameters Affecting the Flow Simulation in the Watershed of Oued Laou (Northern Morocco). *J. Ecol. Eng.* **2019**, *20*, 104–113. [CrossRef]

35. El Khalki, E.M.; Tramblay, Y.; El Mehdi Saidi, M.; Bouvier, C.; Hanich, L.; Benrhanem, M.; Alaouri, M. Comparison of Modeling Approaches for Flood Forecasting in the High Atlas Mountains of Morocco. *Arab. J. Geosci.* **2018**, *11*, 410. [CrossRef]

36. Klemeš, V. Operational Testing of Hydrological Simulation Models. *Hydrol. Sci. J.* **1986**, *31*, 13–24. [CrossRef]

37. Wood, A.W.; Leung, L.R.; Sridhar, V.; Lettenmaier, D.P. Hydrologic Implications of Dynamical and Statistical Approaches to Downscaling Climate Model Outputs. *Clim. Chang.* **2004**, *62*, 189–216. [CrossRef]

38. Fowler, H.J.; Blenkinsop, S.; Tebaldi, C. Linking Climate Change Modelling to Impacts Studies: Recent Advances in Downscaling Techniques for Hydrological Modelling. *Int. J. Climatol.* **2007**, *27*, 1547–1578. [CrossRef]

39. Rosero, E.; Yang, Z.L.; Wagener, T.; Gulden, L.E.; Yatheendradas, S.; Niu, G.Y. Quantifying Parameter Sensitivity, Interaction, and Transferability in Hydrologically Enhanced Versions of the Noah Land Surface Model over Transition Zones during the Warm Season. *J. Geophys. Res. Atmos.* **2010**, *115*, D03106. [CrossRef]

40. Merz, R.; Parajka, J.; Blöschl, G. Time Stability of Catchment Model Parameters: Implications for Climate Impact Analyses. *Water Resour. Res.* **2011**, *47*, W02531. [CrossRef]

41. Seiller, G.; Anctil, F.; Perrin, C. Multimodel Evaluation of Twenty Lumped Hydrological Models under Contrasted Climate Conditions. *Hydrol. Earth Syst. Sci.* **2012**, *16*, 1171–1189. [CrossRef]

42. Gharari, S.; Hrachowitz, M.; Fenicia, F.; Savenije, H.H.G. An Approach to Identify Time Consistent Model Parameters: Sub-Period Calibration. *Hydrol. Earth Syst. Sci.* **2013**, *17*, 149–161. [CrossRef]

43. Coron, L.; Andréassian, V.; Perrin, C.; Bourqui, M.; Hendrickx, F. On the Lack of Robustness of Hydrologic Models Regarding Water Balance Simulation: A Diagnostic Approach Applied to Three Models of Increasing Complexity on 20 Mountainous Catchments. *Hydrol. Earth Syst. Sci.* **2014**, *18*, 727–746. [CrossRef]

44. Ewert, F.; Rötter, R.P.; Bindi, M.; Webber, H.; Trnka, M.; Kersebaum, K.C.; Olesen, J.E.; van Ittersum, M.K.; Janssen, S.; Rivington, M.; et al. Crop Modelling for Integrated Assessment of Risk to Food Production from Climate Change. *Environ. Model. Softw.* **2015**, *72*, 287–303. [CrossRef]

45. Dakhlaoui, H.; Ruelland, D.; Tramblay, Y.; Bargaoui, Z. Evaluating the Robustness of Conceptual Rainfall-Runoff Models under Climate Variability in Northern Tunisia. *J. Hydrol.* **2017**, *550*, 201–217. [CrossRef]

46. Wilby, R.L.; Dessai, S. Robust Adaptation to Climate Change. *Weather* **2010**, *65*, 180–185. [CrossRef]

47. Tramblay, Y.; Ruelland, D.; Somot, S.; Bouaicha, R.; Servat, E. High-Resolution Med-CORDEX Regional Climate Model Simulations for Hydrological Impact Studies: A First Evaluation of the ALADIN-Climate Model in Morocco. *Hydrol. Earth Syst. Sci.* **2013**, *17*, 3721–3739. [CrossRef]

48. Aqnouy, M.; Stitou El Messari, J.E.; Bouadila, A.; Bouizrou, I.; Aoulad Mansour, M.R. Application of Hydrological Model "HEC HMS" in a Mediterranean Watershed (Oued Laou, Northern of Morocco). *Int. J. Innov. Appl. Stud.* **2018**, *24*, 1773–1781.

49. Jakeman, A.J.; Hornberger, G.M. How Much Complexity is warranted in a Rainfall-runoff Model? *Water Resour. Res.* **1993**, *29*, 2637–2649. [CrossRef]

50. Perrin, J.L.; Bouvier, C. Rainfall–runoff modelling in the urban catchment of El Batan, Quito, Ecuador. *Urban Water J.* **2004**, *1*, 299–308. [CrossRef]

51. Perrin, C.; Michel, C.; Andréassian, V. Improvement of a Parsimonious Model for Streamflow Simulation. *J. Hydrol.* **2003**, *279*, 275–289. [CrossRef]

52. Boumenni, H.; Bachnou, A.; Alaa, N.E. The Rainfall-Runoff Model GR4J Optimization of Parameter by Genetic Algorithms and Gauss-Newton Method: Application for the Watershed Ourika (High Atlas, Morocco). *Arab. J. Geosci.* **2017**, *10*, 343. [CrossRef]

53. Salhi, A.; Martin-Vide, J.; Benhamrouche, A.; Benabdelouahab, S.; Himi, M.; Benabdelouahab, T.; Casas Ponsati, A. Rainfall Distribution and Trends of the Daily Precipitation Concentration Index in Northern Morocco: A Need for an Adaptive Environmental Policy. *SN Appl. Sci.* **2019**, *1*, 277. [CrossRef]

54. Kitanidis, P.K.; Bras, R.L. Real-Time Forecasting with a Conceptual Hydrologic Model: 1. Analysis of Uncertainty. *Water Resour. Res.* **1980**, *16*, 1025–1033. [CrossRef]

55. Lamb, R.; Kay, A.L. Confidence Intervals for a Spatially Generalized, Continuous Simulation Flood Frequency Model for Great Britain. *Water Resour. Res.* **2004**, *40*, W07501. [CrossRef]

56. Berthet, L.; Andréassian, V.; Perrin, C.; Javelle, P. How Crucial Is It to Account for the Antecedent Moisture Conditions in Flood Forecasting? Comparison of Event-Based and Continuous Approaches on 178 Catchments. *Hydrol. Earth Syst. Sci.* **2009**, *13*, 819–831. [CrossRef]

57. Brirhet, H.; Benaabidate, L. Comparison of two hydrological models (lumped and distributed) over a pilot area of the Issen watershed in the Souss Basin, Morocco. *Eur. Sci. J.* **2016**, *12*, 347–358. [CrossRef]

58. Benjmel, K.; Amraoui, F.; Aydda, A.; Tahiri, A.; Yousif, M.; Pradhan, B.; Abdelrahman, K.; Fnais, M.S.; Abioui, M. A multidisciplinary approach for groundwater potential mapping in a fractured semi-arid terrain (Kerdous Inlier, Western Anti-Atlas, Morocco). *Water* **2022**, *14*, 1553. [CrossRef]

59. Kostyuchenko, Y.; Artemenko, I.; Abioui, M.; Benssaou, M. Global and Regional Climatic Modeling. In *Encyclopedia of Mathematical Geosciences*; Sagar, B.D., Cheng, Q., McKinley, J., Agterberg, F., Eds.; Springer: Cham, Switzerland, 2022; pp. 1–5. [CrossRef]

60. Aswathi, J.; Sajinkumar, K.S.; Rajaneesh, A.; Oommen, T.; Bouali, E.H.; Binojkumar, R.B.; Rani, V.R.; Thomas, J.; Thrivikramji, K.P.; Ajin, R.S.; et al. Furthering the precision of RUSLE soil erosion with PSInSAR data: An innovative model. *Geocarto Int.* **2022**, *37*, 16108–16131. [CrossRef]

61. Kastridis, A.; Theodosiou, G.; Fotiadis, G. Investigation of Flood Management and Mitigation Measures in Ungauged Natura Protected Watersheds. *Hydrology* **2021**, *8*, 170. [CrossRef]

62. Ikirri, M.; Boutaleb, S.; Ibraheem, I.M.; Abioui, M.; Echogdali, F.Z.; Abdelrahman, K.; Id-Belqas, M.; Abu-Alam, T.; El Ayady, H.; Essoussi, S.; et al. Delineation of Groundwater Potential Area using an AHP, Remote Sensing, and GIS Techniques in the Ifni Basin, Western Anti-Atlas, Morocco. *Water* **2023**, *5*, 1436. [CrossRef]

63. Echogdali, F.Z.; Boutaleb, S.; Kpan, R.B.; Ouchchen, M.; Id-Belqas, M.; Dadi, B.; Ikirri, M.; Abioui, M. Spatialization of flood hazard using Flood Hazard Index method and hydrodynamic modeling tools in a semi-arid environment: A case study of Seyad basin, south of Morocco. *J. Afr. Earth Sci.* **2022**, *196*, 104709. [CrossRef]

64. Mohammadi, B.; Safari, M.J.S.; Vazifehkhah, S. IHACRES, GR4J and MISD-based multi conceptual-machine learning approach for rainfall-runoff modeling. *Sci. Rep.* **2022**, *12*, 12096. [CrossRef]

65. Clarke, R. A review of some mathematical models used in hydrology, with observations on their calibrations and their use. *J. Hydrol.* **1973**, *19*, 1–20. [CrossRef]

66. Nash, J.E.; Sutcliffe, J.V. River Flow Forecasting through Conceptual Models Part I—A Discussion of Principles. *J. Hydrol.* **1970**, *10*, 282–290. [CrossRef]

67. Golmohammadi, G.; Prasher, S.; Madani, A.; Rudra, R. Evaluating Three Hydrological Distributed Watershed Models: MIKE-SHE, APEX, SWAT. *Hydrology* **2014**, *1*, 20–39. [CrossRef]

68. Moriasi, D.N.; Arnold, J.G.; van Liew, M.W.; Bingner, R.L.; Harmel, R.D.; Veith, T.L. Model evaluation guidelines for systematic quantification of accuracy in watershed simulations. *Trans. ASABE* **2007**, *50*, 885–900. [CrossRef]

69. Sinha, A.; Nikhil, S.; Ajin, R.S.; Danumah, J.H.; Saha, S.; Costache, R.; Rajaneesh, A.; Sajinkumar, K.S.; Amrutha, K.; Johny, A.; et al. Wildfire risk zone mapping in contrasting climatic conditions: An approach employing AHP and F-AHP models. *Fire* **2023**, *6*, 44. [CrossRef]

70. Gupta, H.V.; Sorooshian, S.; Yapo, P.O. Status of Automatic Calibration for Hydrologic Models: Comparison with Multilevel Expert Calibration. *J. Hydrol. Eng.* **1999**, *4*, 135–143. [CrossRef]

71. Allam, A.; Moussa, R.; Najem, W.; Bocquillon, C. Hydrological cycle, Mediterranean basins hydrology. In *Water Resources in the Mediterranean Region*; Elsevier: Amsterdam, The Netherlands, 2020; pp. 1–21. [CrossRef]

72. Gu, H.H.; Yu, Z.B.; Yang, C.G.; Ju, Q.; Lu, B.H.; Liang, C. Hydrological Assessment of TRMM Rainfall Data over Yangtze River Basin. *Water Sci. Eng.* **2010**, *3*, 418–430. [CrossRef]

73. Tauro, F.; Selker, J.; Van De Giesen, N.; Abrate, T.; Uijlenhoet, R.; Porfiri, M.; Manfreda, S.; Caylor, K.; Moramarco, T.; Benveniste, J.; et al. Measurements and Observations in the XXI Century (MOXXI): Innovation and Multi-Disciplinarily to Sense the Hydrological Cycle. *Hydrol. Sci. J.* **2018**, *63*, 169–196. [CrossRef]

74. Elbadaoui, K.; Mansour, S.; Ikirri, M.; Abdelrahman, K.; Abu-Alam, T.; Abioui, M. Evaluating the Accuracy of EPM and PAP/RAC in Predicting Soil Erosion in Mountainous Watersheds: An Analysis of the Toudgha River Basin in Southeast Morocco. *Land* **2023**, *12*, 837. [CrossRef]

75. Bhagya, S.B.; Sumi, A.S.; Balaji, S.; Danumah, J.H.; Costache, R.; Rajaneesh, A.; Gokul, A.; Chandrasenan, C.P.; Quevedo, R.P.; Johny, A.; et al. Landslide susceptibility assessment of a part of the Western Ghats (India) employing the AHP and F-AHP models and comparison with existing susceptibility maps. *Land* **2023**, *12*, 468. [CrossRef]

76. Laganier, O.; Ayral, P.A.; Salze, D.; Sauvagnargues, S. A Coupling of Hydrologic and Hydraulic Models Appropriate for the Fast Floods of the Gardon River Basin (France). *Nat. Hazards Earth Syst. Sci.* **2014**, *14*, 2899–2920. [CrossRef]

77. Tzoraki, O.; Cooper, D.; Kjeldsen, T.; Nikolaidis, N.P.; Gamvroudis, C.; Froebrich, J.; Querner, E.; Gallart, F.; Karalemas, N. Flood Generation and Classification of a Semi-Arid Intermittent Flow Watershed: Evrotas River. *Int. J. River Basin Manag.* **2013**, *11*, 77–92. [CrossRef]

78. Norton, A.J.; Rayner, P.J.; Wang, Y.P.; Parazoo, N.C.; Baskaran, L.; Briggs, P.R.; Haverd, V.; Doughty, R. Hydrologic Connectivity Drives Extremes and High Variability in Vegetation Productivity across Australian Arid and Semi-Arid Ecosystems. *Remote Sens. Environ.* **2022**, *272*, 112937. [CrossRef]

79. Ayele, G.T.; Teshale, E.Z.; Yu, B.; Rutherford, I.D.; Jeong, J. Streamflow and Sediment Yield Prediction for Watershed Prioritization in the Upper Blue Nile River Basin, Ethiopia. *Water* **2017**, *9*, 782. [CrossRef]

80. Ragab, R.; Prudhomme, C. SW—Soil and Water: Climate Change and Water Resources Management in Arid and Semi-Arid Regions: Prospective and Challenges for the 21st Century. *Biosyst. Eng.* **2002**, *81*, 3–34. [CrossRef]

81. Ambroggi, R. Etude Géologique du Versant Meridional du Haut Atlas Occidental et de la Plaine du Souss. *Notes Mem. Serv. Géol. Maroc* **1963**, *206*, 37–116.

82. Abioui, M.; Ikirri, M.; Boutaleb, S.; Faik, F.; Wanaim, A.; Id-Belqas, M.; Echogdali, F.Z. GIS for Watershed Characterization and Modeling: Example of the Taguenit River (Lakhssas, Morocco). In *Water, Land, and Forest Susceptibility and Sustainability: Geospatial Approaches and Modeling*; Chatterjee, U., Pradhan, B., Kumar, S., Saha, S., Zakwan, M., Eds.; Elsevier: Amsterdam, The Netherlands, 2023; pp. 61–85. [CrossRef]

83. De Waele, J.; Martina, M.L.V.; Sanna, L.; Cabras, S.; Cossu, Q.A. Flash Flood Hydrology in Karstic Terrain: Flumineddu Canyon, Central-East Sardinia. *Geomorphology* **2010**, *120*, 162–173. [CrossRef]

84. Tramblay, Y.; Bouvier, C.; Martin, C.; Didon-Lescot, J.F.; Todorovik, D.; Domergue, J.M. Assessment of Initial Soil Moisture Conditions for Event-Based Rainfall-Runoff Modelling. *J. Hydrol.* **2010**, *387*, 176–187. [CrossRef]

85. Jin, H.; Liang, R.; Wang, Y.; Tumula, P. Flood-Runoff in Semi-Arid and Sub-Humid Regions, a Case Study: A Simulation of Jianghe Watershed in Northern China. *Water* **2015**, *7*, 5155–5172. [CrossRef]

86. Li, H.; Bao, S.; Wang, X.; Lv, H. Storm Flood Characteristics and Identification of Periodicity for Flood-Causing Rainstorms in the Second Songhua River Basin. *Water* **2016**, *8*, 529. [CrossRef]

87. Li, B.; Liang, Z.; Zhang, J.; Chen, X.; Jiang, X.; Wang, J.; Hu, Y. Risk Analysis of Reservoir Flood Routing Calculation Based on Inflow Forecast Uncertainty. *Water* **2016**, *8*, 486. [CrossRef]

88. Echogdali, F.Z.; Boutaleb, S.; Abioui, M.; Aadraoui, M.; Bendarma, A.; Kpan, R.B.; Ikirri, M.; El Mekkaoui, M.; Essoussi, S.; El Ayady, H.; et al. Spatial Mapping of Groundwater Potentiality Applying Geometric Average and Fractal Models: A Sustainable Approach. *Water* **2023**, *15*, 336. [CrossRef]

89. Bouizrou, I.; Bouadila, A.; Aqnouy, M.; Gourfi, A. Assessment of remotely sensed precipitation products for climatic and hydrological studies in arid to semi-arid data-scarce region, central-western Morocco. *Remote Sens. Appl. Soc. Environ.* **2023**, *30*, 100976. [CrossRef]